

Bi-directional terahertz emission from gold-coated nanogratings by excitation via femtosecond laser pulses

F. Garwe · A. Schmidt · G. Zieger · T. May · K. Wynne ·
U. Hübner · M. Zeisberger · W. Paa · H. Stafast ·
H.-G. Meyer

Received: 8 July 2010 / Revised version: 22 November 2010 / Published online: 5 February 2011
© Springer-Verlag 2011

Abstract We report on the investigation of terahertz (THz) emission from gold-coated nanogratings (500 nm grating constant) upon femtosecond laser irradiation (785 nm, 150 fs, 1 kHz, ≤ 1 mJ/pulse). Unlike common assumptions, THz emission is not only observed in case of rear side irradiation (through substrate (Welsh et al. in *Phys. Rev. Lett.* 98:026803, 2007; Welsh and Wynne in *Opt. Express* 17:2470–2480, 2009)) of the nanograting, but also in case of front side excitation (through air). Furthermore in both cases, THz emission propagates in the direction of laser beam propagation and reverse. Based on these findings, we suggest a new approach to describe the newly observed phenomena. Using a highly sensitive and fast superconducting transition edge sensor (TES) as calorimeter, it was possible to directly measure the absolute energy of the emitted THz pulses in a defined spectral and spatial range, enabling for the first time a quantitative analysis of the THz emission process.

1 Introduction

Growing interest in the terahertz (THz) region of the electromagnetic spectrum originates from its potential applications

in science [1], industry [2], and security [3]. Consequently, a variety of THz source technologies has emerged, as for example, free electron lasers [4], semiconducting cryogenic lasers [5], and THz radiation via optical parametric generation and optical rectification [6, 7]. Ultrashort pulsed techniques have taken on a prominent position in the field of spectroscopy because of their inherent ability to derive spectra by sampling THz pulses using a fraction of the exciting laser pulse. Recent research focuses on the development of suitable materials or structures allowing a high conversion efficiency from the exciting laser energy to THz pulse energy.

This work focuses on THz emission from gold coated nanogratings in fused silica induced by fs laser pulses, as first investigated by [8]. Applying a new experimental method of ultrasensitive calorimetric detection of individual pulses, THz emission is not only observed—as expected—with the laser passing through fused silica onto the rear side of the gold layer [8, 11] but surprisingly also with the laser hitting directly the gold-coated front surface. For both configurations, THz emission was observed both in laser propagation direction and reverse. In the following, we describe the experimental method used to measure the THz emission in direction of laser propagation and to determine their absolute energy. Conclusions are derived from the observation of both the known case of rear side irradiation and the newly discovered THz emission by front side irradiation.

2 Experimental setup

The experimental setup used for the generation and detection of THz radiation is illustrated in Fig. 1. A regeneratively amplified Ti:sapphire laser provides pulses centered at 785 nm wavelength, with a length of 150 fs and ≤ 1 mJ

F. Garwe (✉) · A. Schmidt · G. Zieger · T. May · U. Hübner ·
M. Zeisberger · W. Paa · H. Stafast · H.-G. Meyer
Institute of Photonic Technology, Jena 07745, Germany
e-mail: frank.garwe@ipht-jena.de
Fax: +49(0)-3641-206499

H. Stafast
Faculty of Physics and Astronomy, Friedrich-Schiller-University,
Jena 07743, Germany

K. Wynne
Department of Physics, SUPA, University of Strathclyde,
Glasgow G4 0NG, Scotland, UK

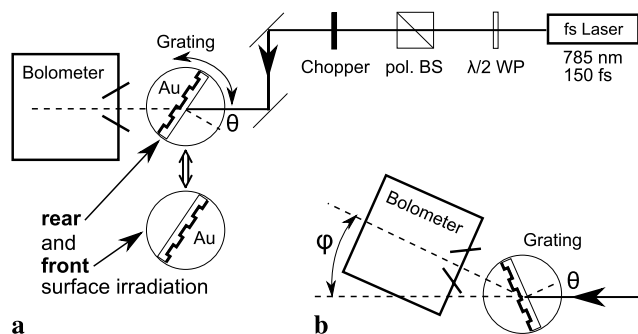


Fig. 1 (a) Scheme of experimental setup for generation and detection of THz radiation: fs laser, $\lambda/2$ wave plate (WP), polarizing beam splitter (BS), chopper, nanograting, and bolometer (b) modified setup for measuring the angular distribution of the THz radiation

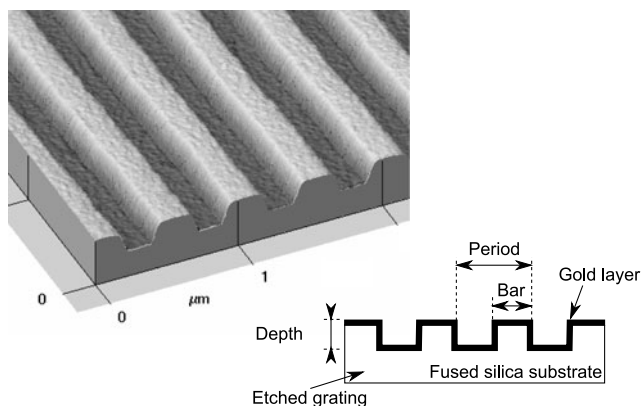


Fig. 2 AFM picture of a gold coated nanograting in fused silica with 500 nm period, 90 nm depth, 250 nm bar width, and 30 nm coating thickness

energy. The linearly polarized laser beam is collimated by a telescope yielding a beam of 5 mm diameter. Its average power is regulated by a $\lambda/2$ wave plate and a polarizer. The angle of incidence θ onto the gold coated grating is varied by rotating the substrate, either with its rear (fused silica) or its front (gold layer) surface oriented toward the laser. The angular distribution (angle φ) of the THz emission is measured in the plane of incidence by moving the detector.

The nanogratings ($5 \times 5 \text{ mm}^2$ area) were produced by 90 nm deep reactive ion etching in UV grade fused silica. The grating constant was 500 nm, whereas the bar width was varied between 250 nm and 320 nm. Using standard thermal evaporation, the gratings were coated with a 30 nm thick gold layer and their geometry measured by an atomic force microscope (AFM) (Fig. 2).

As detector we used a calorimeter based on a superconducting transition edge sensor (TES) [9], which transforms the incident THz pulse to heat by absorbing it in dipole antennas at cryogenic temperatures. Intrinsic electrical heating of the superconductor enables an electrothermal feedback: radiative heating of the detector is compensated by de-

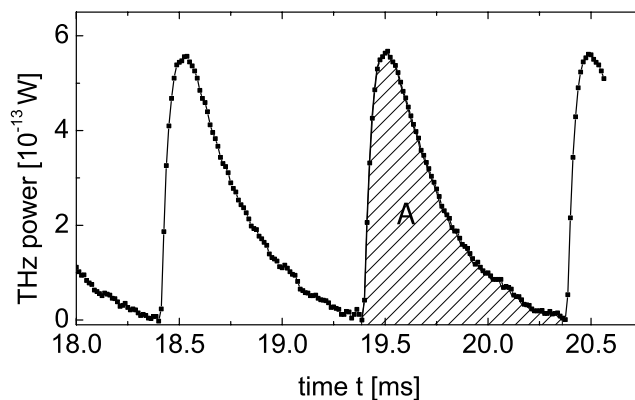


Fig. 3 TES signal showing resolved THz pulses obtained at 0.76 mJ/cm^2 laser pulse fluence; area A corresponds to pulse energy of 0.21 fJ

creased intrinsic heating, which is determined by a current measurement using a cryocooled amplifier providing an output voltage. All visible and infrared radiation except of the intended THz band between 0.34 and 0.38 THz is blocked by a set of filters, which can be easily adapted to other bands in future experiments.

3 Results

Figure 3 illustrates that the TES resolves single THz pulses with a cycle time of 1 ms (1 kHz repetition rate of fs laser). The time integral for an individual pulse (area A) corresponds to its energy, in that case 0.21 fJ. Taking into account the known losses (about 50% due to filter absorption and antenna mismatch), the THz pulse energy in the given spectral and spatial range can be estimated to 0.42 fJ.

Applying this procedure, we measured THz pulse energies for different laser fluences up to 1.3 mJ/cm^2 and both irradiation configurations (Fig. 4). The maximum THz signal was found at an angle of incidence of $\theta_r = (10 \pm 1)^\circ$ for rear side laser irradiation (through silica) and $\theta_f = (8 \pm 1)^\circ$ for front side irradiation. The angular distribution of the THz emission in the plane of laser incidence is displayed in Fig. 5 for both laser irradiation configurations (Fig. 1b) for the example of a grating with 320 nm bar width. The opening angle of the THz emission is about 14° in both cases. The peak of the angular distribution coincides with the direction of the incident laser beam ($\varphi = 0^\circ$).

Taking into account diffraction of the laser beam in the substrate material, the angle of incidence which yields the maximum THz signal is identical in both cases. For both cases, the increase of the THz pulse energy with increasing laser fluence abates at fluences above 1 mJ/cm^2 (Fig. 4). This effect seems to be caused by intrinsic degradation of the grating. It was observed that already fluences above 1.3 mJ/cm^2 cause the THz emission to become smaller in

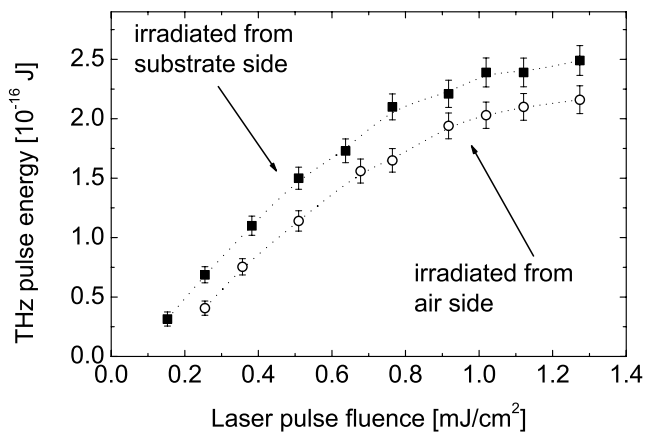


Fig. 4 THz pulse energy as a function of incident laser pulse fluence for both configurations: irradiation of rear (■) and front surface (○)

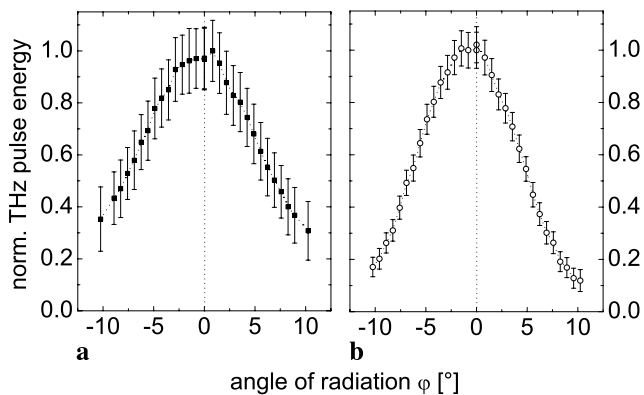


Fig. 5 Normalized THz pulse energy as a function of the emission angle φ obtained with a grating of 320 nm bar width for both laser irradiation configurations: **(a)** rear surface at $\theta_r = (10 \pm 1)^\circ$ **(b)** front surface at $\theta_f = (8 \pm 1)^\circ$; $\varphi = 0^\circ$ is the direction of the laser beam (Fig. 1b)

repeated experiments. Because of that effect the determination of the underlying power law is difficult; however, measurements at low fluences indicate a linear dependence.

The energy of THz pulses upon front side irradiation is about 25% smaller compared to rear side irradiation with the same laser parameters. To support this result, it was confirmed by Fourier transform spectrometry that the transmission through the 1 mm thick fused silica substrate as used for the gratings is $>75\%$ in the 0.34 THz region [10]. In the same spectral range, a transmission measurement of THz radiation through a 30 nm thick gold layer deposited on the same fused silica material reveals that $>99\%$ of the THz radiation is reflected.

These findings suggest that the generated pulse energy in both cases is the same. Thus, the similarity of both observed THz emissions (regarding amplitude, optimum irradiation angle, and spatial distribution) is remarkable.

4 Discussion

The presented experimental findings appear inconsistent with the current model of THz emission [11]. This model is based on field enhancement due to laser excited surface plasmons [12]. It assumes that electrons escape the metal layer upon 3–4 photon absorption processes [13], where they experience ponderomotive forces in the exponentially decaying electric field of the surface plasmons, and thus emit electromagnetic radiation [8].

In our experiment, we provided evidence of THz radiation which explicitly was not generated in the air above the nanograting, since this radiation could hardly be detected through the highly reflective gold film on the grating. On the other hand, electrons escaping from the nanograting into the silica substrate would experience a deceleration which would reduce possible THz emission.

We propose another model, which explains the THz emission without the assumption of free electrons. Surface plasmon polaritons propagating perpendicular to the grooves of the gold grating surface constitute a transient current, which may directly emit THz radiation. Because of the small film thickness, plasmon polaritons on both surfaces strongly couple, resulting in simultaneous emissions from both sides of the grating. The lifetime of such surface plasmon polaritons can be calculated to about several picoseconds using a two temperature model for electrons and phonons [14], which corresponds to the reported length of the THz pulse [11]. This model is supported by our experimental finding that a grating consisting of electrically isolated bars of the gold film does not generate THz radiation. That indicates an interruption of the transient current resulting in a breakdown of THz emission, where the still occurring multiphoton excitations do not significantly contribute to its generation.

5 Conclusion

We reported on the generation of THz pulses induced by femtosecond laser irradiation of gold-coated nanogratings in fused silica. While THz emission via rear side irradiation of the nanograting below the ablation threshold was expected [8, 11], the emission caused by irradiation of the opposite side requires a revision of previous theoretical models. The suggestion that transient currents coming along with the propagation of plasmon polaritons seems to be a promising starting point for future theoretical work. In our next step, we will present in detail further experimental results (paper in preparation) in order to enlarge and improve the basis for theoretical work on the new phenomena.

Furthermore, we have introduced a very sensitive method to determine the absolute energy of single THz pulses. These

energy measurements were performed at 1 kHz repetition rate using a superconductive TES calorimeter. The integration over experimentally measured spatial and spectral distributions of the THz pulse will yield its total energy, allowing for the first time the calculation of the conversion efficiency between an individual femtosecond laser pulse and an individual THz pulse.

Acknowledgements We thank Dr. J. Bergmann from the Institute of Photonic Technology, Jena, Germany, for helpful discussions. The authors acknowledge support by the Thuringian Ministry of Education, Science, and Culture (TeLIGHT, B714-09059).

References

1. M. Brucherseifer, M. Nagel, P. Haring-Bolivar, H. Kurz, A. Bosserhoff, R. Büttner, *Appl. Phys. Lett.* **77**, 4049 (2000)
2. E.J. Heilweil, J.E. Maslar, W.A. Kimes, N.D. Bassim, P.K. Schenck, *Opt. Lett.* **34**, 1360 (2009)
3. T. May, S. Anders, V. Zakosarenko, M. Starkloff, H.-G. Meyer, G. Thorwirth, E. Kreysa, *Proc. SPIE* **6549**, 65490D (2007)
4. M. Sherwin, *Nature* **420**, 131 (2002)
5. E. Bründermann, D. Chamberlin, E. Haller, *Appl. Phys. Lett.* **76**, 2991 (2000)
6. K. Sakai (ed.), *Terahertz Optoelectronics*. Topics in Applied Physics, vol. 97 (Springer, Berlin, 2005)
7. T. Löffler, T. Hahn, M. Thomson, F. Jacob, H. Roskos, *Opt. Express* **13**, 5353 (2005)
8. G. Welsh, N. Hunt, K. Wynne, *Phys. Rev. Lett.* **98**, 026803 (2007)
9. K. Irwin, *Appl. Phys. Lett.* **66**, 1998 (1995)
10. M. Naftaly, R.E. Miles, in *Terahertz Frequency Detection and Identification of Materials and Objects*, ed. by R.E. Miles, X.-C. Zhang, H. Eisele, A. Krotkus (Springer, Dordrecht, 2007), pp. 107–122
11. G. Welsh, K. Wynne, *Opt. Express* **17**, 2470 (2009)
12. Y. Gao, M.-K. Chen, C.-E. Yang, Y.-C. Chang, S. Yin, R. Hui, P. Ruffin, C. Brantley, E. Edwards, C. Luo, *J. Appl. Phys.* **106**, 074302 (2009)
13. J. Kuperszych, *Phys. Rev. Lett.* **95**, 147401 (2005)
14. F. Garwe, U. Bauerschäfer, A. Csaki, A. Steinbrück, K. Ritter, A. Bochmann, J. Bergmann, A. Weise, D. Akimov, G. Maubach, K. König, G. Hüttmann, W. Paa, J. Popp, W. Fritzsche, *Nanotechnology* **19**, 055207 (2008)